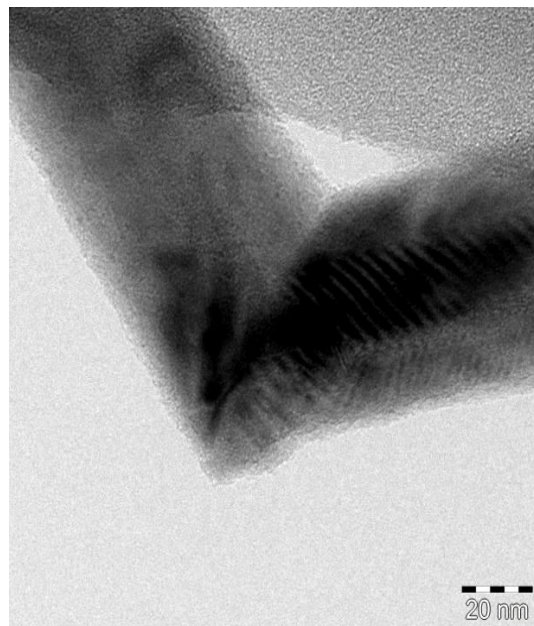


# Synthesis, Characterization and Surface Modification of Titanium and Zinc Oxide Nanostructures for Nanotoxicity, Visible Light Emission and Photocatalytic Studies



Inaugural-Dissertation  
zur Erlangung des Doktorgrades  
der Mathematisch Naturwissenschaftlichen Fakultät  
der Universität zu Köln

vorgelegt von  
Osman Arslan  
aus  
Saruhanli, Manisa/Türkei



Köln, 2013

**Bibliografische Information der Deutschen Bibliothek**

Die Deutsche Bibliothek verzeichnet diese Publikation in der Deutschen Nationalbibliografie; detaillierte bibliografische Daten sind im Internet über <http://dnb.ddb.de> abrufbar.

**Arslan, Osman:**

Synthesis, Characterization and Surface Modification of Titanium and Zinc Oxide Nanostructures for Nanotoxicity, Visible Light Emission and Photocatalytic Studies

ISBN 978-3-86376-132-5

Angefertigt mit Genehmigung der  
Mathematisch-Naturwissenschaftlichen Fakultät der  
Universität zu Köln

Berichterstatter      Prof. Dr. Sanjay Mathur  
                            Prof. Dr. Axel G. Griesbeck  
                            Prof. Dr. Gerd Meyer

Tag der mündlichen Prüfung 12 Dezember 2013

**Alle Rechte vorbehalten**

1. Auflage 2014

© Optimus Verlag, Göttingen

© Coverfoto:

URL: [www.optimus-verlag.de](http://www.optimus-verlag.de)

Printed in Germany

Papier ist FSC zertifiziert (holzfrei, chlorfrei und säurefrei,  
sowie alterungsbeständig nach ANSI 3948 und ISO 9706)

Das Werk, einschließlich aller seiner Teile, ist urheberrechtlich geschützt. Jede Verwertung außerhalb der engen Grenzen des Urheberrechtsgesetzes in Deutschland ist ohne Zustimmung des Verlages unzulässig und strafbar. Dies gilt insbesondere für Vervielfältigungen, Übersetzungen, Mikroverfilmungen und die Einspeicherung und Verarbeitung in elektronischen Systemen.

## Acknowledgements

I want to first thank to my Glorious Allah for giving me patience, perseverance and success and his latest Prophet and Messenger Muhammed Mustafa – Sallallahu Aleyhi ve Sellem- for teaching me how to be a Muslim and Mumin. All comes from Allah – Azze ve Celle- and everyone finds the true salvation in this world and hereafter who understands the Latest Holy Book Qur'an, follows it and the latest Messenger Muhammed Mustafa –Sallallahu Aleyhi ve Sellem- properly. I am extremely thankful to my Ustadh Osman Nuri Topbas (k.s.), his dear friends Ahmed Hamdi Topbas, Abdullah Sert, Dogan Gokmen and proud of being member of such a beautiful Muslim society. Kalbimin Antalya parcasi olan hocalarim Sadik Uzer, Osman Musara, Ramazan Yildiz ve orayi unutulmaz yapan tum agabey ve kardeslerim, Köln'de Lutfi Agabey ve ailesi, Adnan Kurt Agabey ve ailesi, Ibrahim Altun Agabey ve ailesi, Ali Kurt agabey ve ailesi, Atilla Abi ve ailesi, Mustafa Cinar Agabey ve ailesi, Veyis Celik Agabey ve ailesi, Yusuf Agabey (Allah cennetinde bulustursun, amin) ve ailesi, Adnan Sarp Agabey ve ailesi, Gazi Agabey, Muharrem Agabey, Fatih Camurlu Agabey, Timur agabey, Ömer&Ali Agabey, M.Moral agabey, Kenan agabey, M.Taha agabey, Yusuf agabey, Hak Genclik grubumuzun uyeleri, Caglayan Agabey, Murat agabey ve Cuma gününün aksamciları! ve hepsinin aileleri ve isimlerini sayamadigim daha nice saygideger abilerime tesekkur ederim. Siz olmadan bu tez gercektan bir mana ifade etmezdi. Köln sehrini bana cennetten bir bahce yaptiniz!

I am indebted to my friend and advisor Prof. Dr. Sanjay Mathur for inviting me to Germany for this amazing journey into the nanoworld, for our first conversation at March 2009 , giving me the opportunity, encourage, responsibility, amazing guidance, positive criticism, focused commentary, mentorship and freedom to work in this area. I know I am hard to handle but will never forget your inexpressible contribution to my life Professor, thank you so much!

I am grateful to my committee members who helped for the formation of this thesis with their guidance and analysis.

Completion and positive results of this thesis would not have been possible without deep support and help of the members of the Institute of Inorganic and Material Chemistry, and my special thanks go to Dr. Yee Hwa Sehlleier, Dr. Stefan Stucky, Dr. Hao Shen, Dr. Lisong Xiao, Dr. Thomas Rügamer, Linus

Appel, Melanie Hassold, Lisa Czympiel, Mehtap Büyükyazi, Laura Wortmann, Konstantin Konstantynovski, Christopher Waldman, Gregor Fornalczyk, Tessa Leuning, Dr. Mahboube Maleki, Bianka Müller, Thomas Ackermann, Johannes Pfrommer, Ralf Müller, Sebastian Sahler, Dr. Jun Pan, Dr. Aadesh Prataph Singh, Dr. Karthik Raveendran, Dr. Robin von Hagen, Dr. David Zopes, Dr. Irina Giebelhaus, Thomas Fischer, Daniela Hermann, Thomas Lehnen, Michael Kessler, Manuel Langemann, Benjamin Stein, Silke Kremer, Karim Arroub, Anna Jurewicz, Dr. Yakup Gönüllü, Dr. Bilge Saruhan, Martin Hoffman, Roushini Athavale, Peter Golus, Salma Tammam, Andreas Mettenbörger, Nurgül Tosun, Dr. Lhoussaine Belkoura, Dr. X Song, Dr. Ingo Pantenburg, Corinna Hegemann, Dr. Raquel Fiz, Dr. Wieland Tyrra, Shifa Siribbal, Dr. Frank Heinrich, Frau A. Roth, Frau A. Uhlemann, Frau C. Schaefers for their great help and Dr. Abdusalam Uheida, Terrance Burks, Dr. Jingwen Shi, Prof. Dr. Valerian Kagan, Prof. Dr. Harald Krug, Dr. Tina Thurnberr, Prof. Dr. Andrea Kuzmann, Dr. Soile Tuomela, Prof. Dr. Bengt Fadeel and all the other members of NANOMMUNE Project for forming such a great scientific atmosphere. I also express my sincere gratitude to Prof. Dr. Suprakas S. Ray, Dr. Manfred Scriba and other friendly members of CSIR. Thomas, Bonex, Charity, Ella, Sharon, Malcolm, Dr. James, Vuyiswa, Kelso, Simphiwe, Dr. Sreejarani, Dr. Jayita, Dr. David, Dr. Gugu and other unmentioned members of CSIR, thank you that you have provided an amazing environment for me during my stay. Nagi my brother, thank you man but I mean really thank you! I want to thank to Dr. Muhammed Sajid Hussain for Confocal Microscopy measurements, Dr. Dirk Hertel for fluorescence spectroscopy measurements, Ashish Lepcha for being so friendly, Shaista Ilyas for her great help, corrections and support, Prof. Ruschewitz, Klein and Meyer group members for their kind help, Kathrin Stirnat for EPR measurements, Johannes Schlafer for HR-TEM measurements, Dr. Trilok for his extra help and guidance, Dr. Alaeddin Gad for his friendship and humour, Dr J. Li for sharing my laboratory. Thank you Mesude, Yusuf, Okan, Dino and Annika for teaching me!

Thanks to other forgotten friends who helped during this thesis. You were all great!

Babam Abdullah Mesut Arslan

Annem Serife Arslan

Kardeslerim Fatma Betül Arslan,

Meryem Sümeyye Arslan

ve

Yusuf Sami Arslan icin





## **Abstract**

Size dependent quantum confinement and differential characteristics of the anisotropic ZnO and TiO<sub>2</sub> nanomaterials have attracted huge interest in the quest of new functional materials. In order to synthesize ZnO QD's for visible light emission applications, surface modulation for stability in dispersions and defect control at the surface is vitally important. Therefore long alkyl chain group (e.g. oleate) and biological molecule cysteine were used as vectors to regulate reactivity of the ZnO QD's and their visible light emission. Sol-gel chemistry serves as a versatile tool for the fabrication of controlled synthesis of quantum dots and to modify their properties for emission applications such as cell labeling, cell toxicity, solid-state light emission and to understand size/property correlation. High temperature liquid phase synthesis methods, namely heating up and hot injection method were applied toward the synthesis of anisotropic ZnO and TiO<sub>2</sub> nanoparticles. Using different ligand concentrations and reaction conditions, semiconductor nanostructures of unusual geometrical shapes were synthesized and characterized. Hexagonal crystal growing habit of ZnO provided unusual geometrically distorted examples of the hexagonal geometry that have not been reported so far in the literature. Furthermore, TiO<sub>2</sub> nanostructures with significant absorption in visible range of the solar spectrum were obtained by hot injection method and nitrogen doping. The rapid injection and decomposition of Ti-precursor and amine enabled to produce self assembled ball like and multibranched structures with remarkable visible range absorption. Utilization of different concentrations for the precursors provided the possibility of band gap engineering for the anisotropic TiO<sub>2</sub> nanostructures.



## Zusammenfassung

Größenabhängige ZnO und TiO<sub>2</sub> anisotroper Nanomaterialien haben ein enormes Interesse bei der Suche nach neuen Funktionalisierten hervorgerufen. Für die Herstellung von ZnO Nanoteilchen „Quantum Dots“ für die Emission sichtbaren Lichts sind Veränderungen der Oberfläche - für die Stabilität in Dispersionen - sowie eine Kontrolle an der Oberflächen vorhandenen Defekte von wesentlicher Bedeutung. Zu diesem Zwecke wurden ZnO Nanopartikeln durch Einbringung von langkettige Alkyl-Gruppen (z. B. Oleate) sowie biologisch relevante Molekülen wie Cystein modifizierte, um die Reaktivität der ZnO „Quantum Dots“ und deren Emission seigen von sichtbarem Licht zu regulieren. Sol-Gel Prozesse dienen dabei als vielseitige Werkzeuge zur gezielten Synthese von Nanoskaligen Materialen und zum Modifizieren der Eigenschaften für die jeweiligen Anwendungen wie zum Beispiel für die Emission wie die Markierung von Zellen, Photokatalysator und UV- Absorber. Hochtemperaturmethoden in flüssiger Phase wie gezieltes Aufheizen und „Hot Injection“ wurden in dieser Arbeit, zur Synthese Kristallbau ZnO und TiO<sub>2</sub> Nanopartikel angewendet. Durch Verwendung unterschiedlicher Ligandenkonzentrationen und Reaktionsbedingungen konnten Halbleiter-Nanostrukturen in ungewöhnlichen geometrischen Formen erzeugt und charakterisiert werden. Die Kontrolle der Kristallwachstumprozesse von ZnO Nanostrukturen ermöglichte es, ungewöhnliche Morphologien zu erzeugen, die bisher in der Literatur noch nicht beschrieben wurden. Des Weiteren wurden TiO<sub>2</sub>-Nanostrukturen durch die „Hot injection“-Methode erhalten, die eine signifikante Absorption auf Grund einer N-dotierung in sichbaren Bereich aufweisen. Die äußerst schnelle Injektion und spontane Zersetzung des Ti-haltigen Präkursors in Gegenwart eines Amins erlaubte die Darstellung selbstangeordneter Kugelartiger und verzweigter Standformiger Sternförmiger Strukturen mit bemerkenswerten Absorptionen im Bereich des sichtbaren Lichtes. Das Nutzen unterschiedlicher Präkursor-Konzentrationen ermöglicht den gezielten Aufbau anisotroper TiO<sub>2</sub>-Nanostrukturen mit variabler Bandlücken.



## Table of Contents

<b>List of Figures</b>	VII
<b>List of Tables</b>	XVII
<b>Abbreviations and Symbols</b>	XIX
1 Introduction	1
1.1 Nanomaterials: Opportunities and Challenges.....	1
1.2 Scope .....	1
2 State-of-the-Art: Nanostructure Synthesis	5
2.1 General Concepts of Nanostructure Fabrication.....	5
2.1.1 Bottom-up and Top-down Method .....	5
2.2 La-Mer Theory for the Nanoparticle Formation: Nucleation and Growth.....	6
2.2.1 Growth of the Nanoparticles.....	9
2.2.2 Ostwald Ripening.....	10
2.3 Kinetic versus Thermodynamic Control of Anisotropic Particles.....	11
2.3.1 Seed-Mediated Solution–Liquid–Solid (SLS) Growth.....	11
2.3.2 Oriented Attachment .....	12
2.3.3 Kinetically Induced Anisotropic Growth.....	13
2.3.3.1 Surface Energy and Selective Adhesion .....	13
2.3.3.2 Influence of the Phase of the Crystalline Seed.....	17
2.3.3.3 Thermodynamic or Kinetic Control of the Growth Regime.....	18
2.4 Nano-Synthetic Methods.....	21
2.4.1 Hot Injection Synthesis .....	21
2.4.2 Heating Up Method for Nanostructures.....	22
2.4.3 Sol Gel Method for Synthesis .....	23
2.4.3.1 Organically Modified Nanostructures by Sol Gel Method .....	24
2.4.4 Hydro-Solvo Thermal Method for Nanostructures.....	24

---

**Table of Contents**

---

2.5 MOx/Polymer Nanocomposites .....	25
2.5.1 Hybrid Inorganic Organic Polymer/MOx Nanocomposite.....	25
2.5.2 MOx@Clay Nanocomposite Structures .....	27
3 Experimental Part	29
3.1 Experimental Procedures .....	29
3.1.1 Synthesis of ZnO Nanostructures .....	29
3.1.1.1 Salt Elimination Method for Zn(Oleate) <sub>2</sub> .....	30
3.1.1.2 Amide Method for Zn(Oleate) <sub>2</sub> Precursor.....	30
3.1.2 Ligand Controlled ZnO Quantum Dot Synthesis .....	31
3.1.2.1 Acetate Controlled ZnO QD Synthesis .....	31
3.1.2.2 Cysteine Capped Zwitterionic ZnO QD Synthesis .....	32
3.1.2.3 Oleate Capped ZnO QD Synthesis.....	32
3.1.2.4 Phase Transfer Synthesis of ZnO QD's .....	32
3.1.3 Heating Up Synthesis of Anisotropic ZnO Nanoparticles.....	33
3.1.3.1 Salt Assisted Surface Modification of ZnO Nanostructures.....	34
3.1.3.2 SiO <sub>2</sub> @ZnO Core/Shell (Encapsulated) Nanostructures with Different Surface Modifications .....	35
3.1.4 Synthesis of TiO <sub>2</sub> Nanostructures .....	36
3.1.4.1 Synthesis of one-dimensional TiO <sub>2</sub> Nanofibers by Hydrothermal Method .....	37
3.1.4.2 Synthesis of Spherical TiO <sub>2</sub> Nanoparticles by Heating Up Method.....	38
3.1.4.3 Synthesis of Multibranched, Elongated TiO <sub>2</sub> Nanostructures by Hot Injection Method .....	38
3.1.5 Inorganic Organic Hybrid Polymer/ZnO Nanocomposite Synthesis .....	39
3.1.5.1 PLA/Hybrid Polymer/NP Nanocomposite Synthesis .....	41
3.1.5.2 ZnO@Clay Nanocomposite Preparation.....	42
3.2 Characterization Techniques.....	42

---

**Table of Contents**

3.2.1 Transmission and High Resolution Transmission electron Microscopy.....	42
3.2.2 Scanning Electron Microscopy (SEM) and Electron Diffraction X-Ray (EDX) .....	43
3.2.3 X-Ray Diffraction Spectroscopy.....	43
3.2.4 Thermogravimetric Analysis .....	44
3.2.5 Atomic Force Microscopy (AFM) .....	44
3.2.6 Photoluminescence Spectroscopy .....	44
3.2.7 UV-Visible Spectroscopy .....	44
3.2.8 Surface Contact Angle .....	45
3.2.9 Dynamic Light Scattering (DLS).....	45
3.2.10 Zeta Potential Measurements .....	45
3.2.11 FT-Infrared Spectroscopy .....	45
3.2.12 NMR Spectroscopy .....	46
3.2.13 Confocal Microscopy .....	46
3.3 Material Properties Testing .....	46
3.3.1 Cell Cytotoxicity Tests.....	46
3.3.2 Cell Labeling by Visible Light Emitting QD's.....	47
3.3.3 Photocatalytic Activity Tests .....	47
<b>4 Results and Discussion</b>	<b>51</b>
4.1 Ligand Modulated Visible Light Emitting ZnO QD's.....	51
4.1.1 Fundamental Properties of ZnO QD's and Their Visible Light Emission .....	51
4.1.2 Acetate as Controlling Ligand for ZnO QD' s .....	52
4.1.2.1 UV-Visible Investigation and Particle Size Calculation.....	53
4.1.2.2 Photoluminescence Properties and Visible Light Emission .....	54
4.1.3 Cysteine Molecule as Surface Controlling Ligand for ZnO QD's .....	56
4.1.3.1 Optical Evolution and Band Gap Modulation of ZnO QD Formation under Cysteine Control.....	57

---

**Table of Contents**

4.1.3.2 Real Crystal Size, Morphology and Surface Properties of Cystein@ZnO QD's .....	60
4.1.3.3 PL Features and Stability of Cysteine Modified ZnO QD's .....	63
4.1.3.4 Cysteine Triggered Self Assembly in the ZnO QD's .....	68
4.1.4 Ultrastable Oleate@ZnO QD's for Phase Transfer and Storage .....	70
4.1.4.1 General and Swift Synthesis of Blue to Yellow Visible Light Emitting Oleate@ZnO QD's .....	71
4.1.4.2 NMR Measurements for Identification of Oleate Ligand .....	79
4.1.4.3 Ultrastability and Agglomeration Free Feature of Oleate@ZnO QD's .....	81
4.1.4.4 Phase Transfer Synthesis for Water Soluble ZnO QD's and Other Techniques for Visible Light Emission Manipulation .....	87
4.1.5 Nanomaterials and Discussion of Ligand@ZnO QD's .....	92
4.1.5.1 Cytotoxicity and Cell Labeling by Ligand@ZnO QD's .....	92
4.1.5.2 Selective UV-A (400-315 nm) and UV-B (315-280) Region Protection by ZnO QD's and Antibacterial, Transparent, Hybrid Nanocomposites .....	94
4.2 Anisotropic ZnO Nanoparticles by Heating Up Method .....	95
4.2.1 Basics of ZnO Heating Up Method .....	95
4.2.2 Plate like and Pyramidal ZnO Nanoparticles by Heating Up .....	96
4.2.3 Distorted Examples of Anisotropic ZnO Nanoparticles by Heating Up Method .....	98
4.2.4 Crystallinity and Surface Modification of the Anisotropic ZnO Nanostructure .....	106
4.2.5 Optical, Thermal and Aqueous Properties of the Surface Modified ZnO Nanocrystals .....	108
4.2.6 Ligand@ZnO Nanostructures as Nanobiotechnology Nanomaterials .....	113
4.2.6.1 Ligand Effect for the Nanotoxicity and Gene Regulation .....	113

---

**Table of Contents**

4.2.6.2 Cell Labeling by Fluorescein Modified ZnO Nanoplates .....	115
4.2.6.3 Photocatalytic activity of the Nanostructures for the Decomposition of Methylene Blue .....	116
4.3 Synthesis of Visible Light Active, Multibranched TiO <sub>2</sub> Nanostructures by Hot Injection Method.....	118
4.3.1 Thermogravimetric Analysis of TiO <sub>2</sub> Precursor for Hot Injection Method .....	119
4.3.2 Visible Light Active Spherical TiO <sub>2</sub> by Hot Injection Method .....	121
4.3.2.1 Synthesis and Morphology Investigation of Visible Light Active Spherical TiO <sub>2</sub> .....	122
4.3.2.2 Band Gap Calculation of Spherical TiO <sub>2</sub> Nanostructures.....	124
4.3.3 Crystallinity, Surface and Thermal Properties.....	124
4.3.4 Visible Light Active, Multibranched TiO <sub>2</sub> NR by Hot Injection Method .....	126
4.3.4.1 Synthesis and Crystallinity of Visible Light Active Multibranched TiO <sub>2</sub> Nanostructures .....	127
4.3.4.2 TEM Investigation of the Multibranched, Visible Light Active TiO <sub>2</sub> .....	128
4.3.4.3 Fundamental Nanorod Morphology for the TiO <sub>2</sub> Nanostructures.....	129
4.3.4.4 Angle Between the Attaching Nanorods.....	133
4.3.4.5 Possible Formation Mechanism for the TiO <sub>2</sub> Multibranched Nanostructures .....	135
4.3.4.6 Nanomaterial Applications of Spherical and Multibranched Visible Light Active TiO <sub>2</sub> Nanostructures .....	138
4.3.5 Solar Light Driven Photocatalysis of Visible Light Active TiO <sub>2</sub> ....	138
4.4 Metal Oxide / Polymer Nanocomposites .....	140
4.4.1 Hybrid Inorganic Organic Polymer/MOx Nanocomposites .....	140
4.4.1.1 TiO <sub>2</sub> Nanowire/Epoxy-amine Superhydrophilic Nanocomposite .....	141
4.4.2 Polymer and ZnO QD Nanocomposites .....	142

## **Table of Contents**

---

4.4.2.1 Selective UV Protective Transparent ZnO/Hybrid Nanocomposites .....	143
4.4.3 Biodegradable PLA/Metal Oxide Nanocomposites.....	144
4.4.3.1 PLA/MEMO/ZnO QD Nanocomposites.....	144
4.4.4 ZnO QD@Clay Nanocomposites For Light Emitting Clays .....	151
5 Conclusions and Outlook	153
5.1 Conclusions .....	153
5.2 Outlook and Future Prospects .....	155
References	157
Ehrenwörtliche Erklärung	169
Curriculum Vitae	170

## List of Figures

<b>Figure 1</b>	General ZnO and TiO <sub>2</sub> nanostructure synthesis .....	2
<b>Figure 2</b>	Ligand library for the surface modification and core/shell protection of the nanoparticles.....	3
<b>Figure 3</b>	Several applications of ZnO and TiO <sub>2</sub> nanostructures. ....	4
<b>Figure 4</b>	Scheme of complementary “top-down” and “bottom-up” approaches for fabrication of micro- and nano-structures <sup>[19]</sup> .....	5
<b>Figure 5</b>	Schematic diagram illustrating La Mer’s condition for stable nucleation <sup>[39]</sup> .....	6
<b>Figure 6</b>	Free energy diagramme explaining the critical nucleus <sup>[40]</sup> .....	8
<b>Figure 7</b>	Schematic of nucleation and growth of the nanocrystals in La Mer theory <sup>[41]</sup> .....	9
<b>Figure 8</b>	Sketch of Ostwald ripening process <sup>[43]</sup> .....	10
<b>Figure 9</b>	Alloy formation of the solution grown nanowires <sup>[45]</sup> .....	12
<b>Figure 10</b>	Schematic representation of oriented attachment processes <sup>[45]</sup> .....	13
<b>Figure 11</b>	Surface energy of wurtzite ZnS nanocrystals. ....	14
<b>Figure 12</b>	Surface modulation effects induced by surface-selective surfactants on either a) anisotropic rod or b) disc growth. ....	15
<b>Figure 13</b>	Shape evolution of TiO <sub>2</sub> nanocrystals through the surface energy modulation effect by using surface selective lauric acid (LA) surfactants. ....	16
<b>Figure 14</b>	Temperature-mediated crystalline-phase control of a,b) MnS and c,d) CdS nanocrystals.....	18
<b>Figure 15</b>	a,b) Heterostructured rods formed by adding CdSe extensions to each end of CdS nanorods. c,d) Branched rods result from the nucleation of zinc blende CdTe on either end of the CdSe nanorods(continues).....	19
<b>Figure 16</b>	Comparison of a) thermodynamic and b) kinetic growth of PbS nanocrystals.....	20
<b>Figure 17</b>	Experimental set-up and reaction scheme for the hot-injection method <sup>[49]</sup> .....	22

---

**Table of Contents**

<b>Figure 18</b> Basic reactions of sol gel method from a metal alkoxide.....	23
<b>Figure 19</b> Morphological variation schema for sol-gel method <sup>[52]</sup> .....	23
<b>Figure 20</b> Solvo/hydrothermal synthesis installation <sup>[54]</sup> .....	25
<b>Figure 21</b> Example of a hybrid formulation consisting of acrylic alkoxysilane, biodegradable PLA and ZnO QD's. ....	26
<b>Figure 22</b> Idealized structure montmorillonite clay (without organic modification) showing two tetrahedral-site sheets fused to an octahedral-site sheet.....	27
<b>Figure 23</b> Exfoliated (left) and intercalated (right) clay structures by polymeric architectures.....	28
<b>Figure 24</b> Würzite crystal structure of ZnO. ....	29
<b>Figure 25</b> Amide procedure of ZnO QD synthesis from an organometallic precursor. ....	31
<b>Figure 26</b> Non hydrolytic high temperature formation mechanism of ZnO nanoparticles from oleate precursor.....	33
<b>Figure 27</b> Experimental set-up for the heating up method for ZnO nanocrystal synthesis. ....	34
<b>Figure 28</b> General carboxylic acid modification of ZnO nanoparticles.....	35
<b>Figure 29</b> Crystal structures of TiO <sub>2</sub> phases and atomic orientation in the TiO <sub>2</sub> crystal structures.....	37
<b>Figure 30</b> Spherical TiO <sub>2</sub> formation by Hot Injection method. ....	38
<b>Figure 31</b> Hot Injection Synthesis of Multibranched TiO <sub>2</sub> . ....	39
<b>Figure 32</b> Partial hydrolysis of epoxy modified trialkoxysilane.....	40
<b>Figure 33</b> Epoxy ring opening reactions in hybrid nanocomposites. ....	41
<b>Figure 34</b> Schema for the nanoparticle surface modification. ....	41
<b>Figure 35</b> MTT test for the cell viability.....	46
<b>Figure 36</b> Photocatalytic process for the formation of charge carriers of TiO <sub>2</sub> <sup>[86]</sup> .....	48
<b>Figure 37</b> Photoluminescent processes suggested for ZnO nanoparticles <sup>[97]</sup> .....	52
<b>Figure 38</b> UV Visible evolution of Acetate@ZnO QD's.....	53

---

**Table of Contents**

<b>Figure 39</b> a) TEM investigation of Acetate@ZnO QD's b) QD size distribution.....	54
<b>Figure 40</b> Visible green emission from the Acetate@ZnO QD's (aliquot times have been written in minutes below the solution).....	54
<b>Figure 41</b> PL spectra for the QD's before and after storage.....	55
<b>Figure 42</b> Green to orange light shift for Acetate@ZnO QD's.....	55
<b>Figure 43</b> Acetate@ZnO QD agglomeration and monolayer formation. ....	56
<b>Figure 44</b> Cysteine-functionalized ZnO QDs and intermolecular interaction among surface-bound and free cysteine ligands.....	57
<b>Figure 45</b> UV visible Evolution of the Cysteine @ ZnO QD's. ....	57
<b>Figure 46</b> Band gap calculation of the ZnO quantum dot.....	58
<b>Figure 47</b> Band gap variation of Cysteine@ZnO QD's.....	59
<b>Figure 48</b> Particle size evolution for the formation of Cysteine@ZnO QD's. ....	60
<b>Figure 49</b> TEM images and calculated particle size distribution of Cysteine@ZnO QD's.....	61
<b>Figure 50</b> XRD patterns of C1,C2,C3 and Acetate@ZnO QD's. ....	61
<b>Figure 51</b> FTIR spectra of (a) free cysteine, (b) C0, (c) C3, (d) C2, and (e) C1 samples.....	62
<b>Figure 52</b> Cysteine (C1) modified ZnO QD's visible light emission. ....	63
<b>Figure 53</b> Photoluminescence feature of C2 QD's.....	63
<b>Figure 54</b> Photoluminescence stability of Cysteine@ZnO QD's, before (left solution) and after (right solution) 1 week (C3). ....	64
<b>Figure 55</b> Fluorescence lifetime and automatic correction of cysteine capped ZnO QD's (C3).....	65
<b>Figure 56</b> EDX analysis and SEM images of the C1, C2 and C3.....	66
<b>Figure 57</b> TGA investigation of Acetate@ZnO and C3. ....	66
<b>Figure 58</b> TG-DTA analysis of pure cysteine, C1 and C2. ....	67
<b>Figure 59</b> Zeta potential measurements for Acetate@ZnO and Cysteine@ZnO.....	68

<b>Figure 60</b> Assembly of ZnO QDs to form supra-structures and their hydrodynamical property observation with time.....	69
<b>Figure 61</b> Hydrodynamic size variation before and after self assembly.....	70
<b>Figure 62</b> Synthesis of Oleate@ZnO QD's by modified sol-gel method.....	72
<b>Figure 63</b> Evolution of the optical properties of Oleate@ ZnO QD's (ZnO-1). .....	73
<b>Figure 64</b> TEM, HR-TEM and SAED patterns of ZnO-1.....	75
<b>Figure 65</b> Size distributions in Oleate@ZnO nanoparticles.....	75
<b>Figure 66</b> Visible light emission characteristics of ZnO-1. ....	76
<b>Figure 67</b> Visible emissions of a)ZnO-2, b)ZnO-3 and c)Acetate@ZnO.....	77
<b>Figure 68</b> Optical properties of ZnO-2, ZnO-3 ve ZnO-4, Inset images represent visible emission colour of the quantum dots.....	78
<b>Figure 69</b> $^1\text{H}$ NMR for the $\text{Zn}(\text{Oleate})_2$ precursor.....	79
<b>Figure 70</b> NMR investigation of ZnO quantum dot precursor $\text{Zn}(\text{Oleate})_2$ .....	79
<b>Figure 71</b> FT-IR observation of transformation of molecular precursor in the Oleate@ZnO QD. .....	80
<b>Figure 72</b> NMR investigation of Oleate@ZnO QD's. ....	81
<b>Figure 73</b> Core-shell structure of the Oleate@ZnO QD's for the synthesized Oleate@QD's. ....	82
<b>Figure 74</b> TEM and HR TEM images of ZnO-2 (left) and ZnO-3 right.....	83
<b>Figure 75</b> TEM investigation of oleate removal for ZnO-1.....	83
<b>Figure 76</b> XRD patterns of ZnO-1 before and after heat treatment. ....	84
<b>Figure 77</b> XRD patterns of the Acetate@ZnO and ZnO-2, ZnO-3.....	84
<b>Figure 78</b> Comparison of the agglomeration behavior of a b)Acetate@ZnO and c-d) Oleate@ZnO QD's. ....	85
<b>Figure 79</b> Stability observation of the Oleate@ZnO QD'in in EtOH (a-b-c) and $\text{CHCl}_3$ (d-e-f) during 6 month with their TEM analysis after storage.....	86
<b>Figure 80</b> TGA analysis of oleate loading for ZnO QD's.....	87

---

**Table of Contents**

<b>Figure 81</b> a)Oleate@ZnO QD's to Gluconic@ZnO QD b)Appearance before and phase transfer under UV illumination ( $\lambda_{\text{max}}= 354$ nm) c) TEM images before and after phase transfer with gluconic acid .....	88
<b>Figure 82</b> FT-IR confirmation of the phase transfer for gluconic acid .....	89
<b>Figure 83</b> Salt like attachment of gluconate after phase transfer synthesis. ....	89
<b>Figure 84</b> ZnO QD's solutions for different visible light emissions.....	90
<b>Figure 85</b> Silica encapsulation causes quenching in visible light emission. ....	91
<b>Figure 86</b> a) Confocal images of the HEK cells after 2h incubation b) MTT test for the cell viability during 4h with different dosing.....	93
<b>Figure 87</b> Cysteine capped ZnO cell labeling and cytotoxicity. ....	94
<b>Figure 88</b> Thermal decomposition profiles of precursor mixtures.....	96
<b>Figure 89</b> Decomposition mechanism of ZnO precursor and FT-IR observation .....	97
<b>Figure 90</b> FT-IR spectra for the comparison of beginning and final composition.....	98
<b>Figure 91</b> Nanoplate morphology for the ZnO nanoparticles. ....	98
<b>Figure 92</b> TEM investigation of the nanoplates diameter and length. ....	99
<b>Figure 93</b> Hexagonal morphology of the ZnO nanocrystals. ....	100
<b>Figure 94</b> Distorted hexagonal nanocrystals of the ZnO. ....	101
<b>Figure 95</b> Particle size distribution of the ZnO-distorted hexagonal nanoparticles. ....	102
<b>Figure 96</b> Particle size distribution of the pyramid like ZnO NP's.....	102
<b>Figure 97</b> TEM investigation of the pyramidal ZnO nanocrystals. ....	103
<b>Figure 98</b> Heart shaped assembly from pyramidal ZnO nanoparticles. ....	103
<b>Figure 99</b> Nanoparticle twins of the pyramidal ZnO NP's. ....	104
<b>Figure 100</b> TEM and particle size investigation of the ZnO nanorods. ....	105
<b>Figure 101</b> XRD pattern of the as-synthesized ZnO Nanorod. ....	106
<b>Figure 102</b> XRD pattern of the nanoplate like ZnO.....	106

---

**Table of Contents**

<b>Figure 103</b> XRD pattern of the pyramidal ZnO .....	107
<b>Figure 104</b> XRD pattern of the distorted hexagonal ZnO nanostructure.....	107
<b>Figure 105</b> FT-IR spectra for the bare ZnO nanocrystals. ....	108
<b>Figure 106</b> FT-IR and UV Vis- absorption spectra of the folic acid modified ZnO Nanorods. ....	109
<b>Figure 107</b> FT-IR and UV –Vis absorption spectra of the citric acid modified nanopyramids. ....	110
<b>Figure 108</b> UV Vis spectrum for the Mandelate@ZnO nanoplate. ....	110
<b>Figure 109</b> NMR spectra for mandelic acid modification of ZnO nanoplates.....	111
<b>Figure 110</b> TEM investigation of the mandelic acid modified ZnO nanoplates.....	111
<b>Figure 111</b> Thermal weight loss of the folic acid modified ZnO nanorods.....	112
<b>Figure 112</b> Thermal decomposition pattern of the citric acid modified ZnO nanopyramids.....	112
<b>Figure 113</b> Schematic representation of some key events of ZnO toxicity in Jurkat cells <sup>[131]</sup> .....	114
<b>Figure 114</b> Increasing amount of dissolution by the increasing amount of zinc species <sup>[131]</sup> .....	115
<b>Figure 115</b> Fluorescein@ZnO nanoplate/nanopyramid cell labeling (bar=10 micrometer). ....	116
<b>Figure 116</b> Photocatalytic activity of ligand modified ZnO nanoparticles ....	117
<b>Figure 117</b> TiO <sub>2</sub> precursor mixture evolution during the hot injection synthesis. ....	119
<b>Figure 118</b> TGA decomposition profile of Ti-precursor mixtures. ....	120
<b>Figure 119</b> FT-IR confirmation of the amide formation until 150 °C. ....	120
<b>Figure 120</b> FT-IR confirmation of the amide formation for the Ti-precursor.....	121
<b>Figure 121</b> Self assembly formation of the spherical TiO <sub>2</sub> nanoparticles. ....	122
<b>Figure 122</b> Self assembly spheres of TiO <sub>2</sub> and their size distribution. ....	123

<b>Figure 123</b> Band Gap calculation and SEM images of TiO <sub>2</sub> nanoparticles and color comparison of spheres with P-25.....	124
<b>Figure 124</b> XRD patterns of the spherical TiO <sub>2</sub> nanoparticles.....	125
<b>Figure 125</b> FT-IR investigation of the spherical TiO <sub>2</sub> nanoparticles.....	125
<b>Figure 126</b> Thermogravimetric analysis and EDX of the spherical TiO <sub>2</sub> nanoparticles. ....	126
<b>Figure 127</b> SEM images of the multibranched TiO <sub>2</sub> nanocrystals and EDX investigation.....	127
<b>Figure 128</b> XRD spectra and color difference of elongated TiO <sub>2</sub> .....	128
<b>Figure 129</b> Schematic perspective of multibranching in the TiO <sub>2</sub> Nanostructures. ....	129
<b>Figure 130</b> Dipod like TiO <sub>2</sub> nanostructures. ....	129
<b>Figure 131</b> Tripod like nanostructures of TiO <sub>2</sub> .....	130
<b>Figure 132</b> Examples of tetrapod like TiO <sub>2</sub> nanostructures. ....	131
<b>Figure 133</b> Obtained multipod TiO <sub>2</sub> Nanostructures. ....	131
<b>Figure 134</b> Fabricated alphabet nanogallery of TiO <sub>2</sub> without size bars.....	132
<b>Figure 135</b> Proximity of the different TiO <sub>2</sub> nanostructures. ....	133
<b>Figure 136</b> Angle distribution between the V shaped dipod structures. ....	133
<b>Figure 137</b> HR-TEM image and SAED pattern of the TiO <sub>2</sub> nanorods. ....	134
<b>Figure 138</b> HR TEM investigation for the junction points. ....	135
<b>Figure 139</b> Shape evolution of TiO <sub>2</sub> nanocrystals through the surface energy modulation effect by using surface selective lauric acid (LA) surfactants <sup>[46]</sup> . ....	136
<b>Figure 140</b> Titanium alkoxide for the elongated nanostructures <sup>[83]</sup> .....	137
<b>Figure 141</b> Distorted truncated and cube like truncated structures in the early stages of nanorod formation. ....	138
<b>Figure 142</b> Solar light spectrum and solar driven visible light photocatalysis.....	138
<b>Figure 143</b> Photocatalytic comparison activity of of P-25, TiO <sub>2</sub> Rod and TiO <sub>2</sub> Spheres by solar light .....	139

---

**Table of Contents**

<b>Figure 144</b> Hybrid nanocomposite preparation techniques left) UV curable right) epoxy amine. ....	140
<b>Figure 145</b> TiO <sub>2</sub> Nanowires by hydrothermal method by self dissolution of TiO <sub>2</sub> nanoparticles. ....	141
<b>Figure 146</b> Superhydrophilic nanocomposite coatings on glass (surface angle < 5°). ....	142
<b>Figure 147</b> %5 (left) and %10 (right) percent ZnO QD containing nanocomposite coatings antibacterial testing. ....	142
<b>Figure 148</b> Antibacterial test for 5% ZnO QD containing nanocomposite against to Pseudomonas Aeruginosa (left) and S. Aureus (right). ....	143
<b>Figure 149</b> PLA/MEMO hybrid nanocomposite preparation. ....	144
<b>Figure 150</b> ZnO QD addition into the PLA/MEMO nanocomposite structures for light emitting nanocomposites. ....	145
<b>Figure 151</b> FT-IR investigation of UV curable PLA/MEMO nanocomposite mixtures. ....	145
<b>Figure 152</b> Effect of UV curing for the PLA/MEMO nanocomposite structure. ....	146
<b>Figure 153</b> Deformation by e-beam for the PLA/%10 MEMO nanocomposite ....	146
<b>Figure 154</b> Change of roughness from PLA/%10 MEMO to PLA/%50 MEMO. ....	146
<b>Figure 155</b> Cross sectional SEM analysis with increasing MEMO content (from %20 to %50 respectively). ....	147
<b>Figure 156</b> Transparency of the %30 MEMO/PLA nanocomposite polymer. ....	148
<b>Figure 157</b> Contact angle increase with increasing MEMO content. ....	148
<b>Figure 158</b> PLA biodegradation with a commercial compost formulation. ....	149
<b>Figure 159</b> Solid state light emitting nanocomposites. ....	149
<b>Figure 160</b> FIB-Back scattering images of metal oxide/PLA for observing particle dispersion. ....	150

---

**Table of Contents**

<b>Figure 161</b> FIB image of liquid N <sub>2</sub> frozen MOx/PLA nanocomposite structure.....	150
<b>Figure 162</b> ZnO QD@Nanorod Clay Nanocomposites. ....	151
<b>Figure 163</b> ZnO QD decoration for the plate like clays.....	152
<b>Figure 164</b> Oleate@ZnO QD's and solid state light emitting nanocomposites.....	153
<b>Figure 165</b> ZnO morphology gallery obtained by heating up method.....	154
<b>Figure 166</b> TiO <sub>2</sub> morphology gallery and HR-TEM of TiO <sub>2</sub> by Hot Injection. ....	155



## List of Tables

<b>Table 1</b>	Synthesis concentrations of Zn-Oleate complex.	30
<b>Table 2</b>	Band gap variation of growing Cysteine@ZnO QD's	59
<b>Table 3</b>	Time dependent particles size variation according to UV visible investigation	60
<b>Table 4</b>	Size, band gap and emission maxima list for ZnO a) Obtained from UV-Vis absorption b) Obtained from effective mass model ( $m_e = 0.26 m_0$ , $m_h = 0.59m_0$ , $m_0$ is the,free electron mass, $\epsilon = 8.5$ , and $E_g$ bulk = 3.3 eV) c)From UV-Vis absorption	74
<b>Table 5</b>	Modification list for the ZnO nanocrystals	108



## **Abbreviations and Symbols**

QD	Quantum Dot
SEM	Scanning Electron Microscopy
TEM	Transmission Electron Microscopy
HR-TEM	High Resolution Electron Microscopy
°C	Degree Celcius
EDX	Energy Dispersive X-Ray Spectroscopy
XRD	X-Ray Diffraction
FT-IR	Fourier Transformed Infra Red
UV –Vis	Ultraviolet- Visible
Raman	Raman Spectroscopy
EPR	Electron Paramagnetic Resonance Spectroscopy
NMR	Nuclear Magnetic Resonance Spectroscopy
DLS	Dynamic Light Scattering
FIB	Focused Ion Beam
PL	Photoluminescence Spectroscopy
μ	Prefix for Micro ( $1.10^{-6}$ m)
AFM	Atomic Force Microscopy
ppm	Parts per million
NP	Nanoparticle
NR	Nanorod
Eg	Band Gap Energy
eqv	equivalent
eV	electron volt
g	Gram
hv	Insident Photon Energy
Θ	Theta (diffraction angle)
h	hour-s
JCPDS	Joint Committee on Powder Diffraction Standards
v <sub>asym</sub>	Asymmetric stretching mode
v <sub>sym</sub>	Symmetric stretching mode
Mol	Mol amount
TGA	Thermogravimetric analysis
λ	Wavelength
nm	suffix for nanometer ( $1.10^{-9}$ m)



# **1 Introduction**

## **1.1 Nanomaterials: Opportunities and Challenges**

Among various metal oxide structures ZnO and TiO<sub>2</sub> have found wide spread applications due to their structural<sup>[1-4]</sup>, electronic<sup>[5-7]</sup> and surface properties<sup>[8-10]</sup>. Generally metal oxide nanomaterials have already begun to effect fundamental characteristics of future materials due to their unique, easy to manipulate and novel performances. Industrial applications of these metal oxides, require established synthesis strategies for scaled up production and detailed investigations of nanoparticles on possible toxicological effects on the living organisms. It is widely experienced that metal oxide nanomaterials, due to nanoparticle anisotropy, quantum confinement effects and surface reactivity need broad attention by an interdisciplinary (the chemical, physical, biological, material science) society. Detailed investigation of these properties, enable the synthesis of programmable nanomaterials which having specific material characteristics like particle size<10 nm, or selectively elongated facets of nanoparticles for better catalytic efficiency<sup>[11-12]</sup>. Since optical and morphological control leads to control of the light emission or defect oriented new properties, extremely sensitive synthesis methods are required to develop long term stable nanostructures. In addition to that catalytic or photocatalytic properties can be improved by fine control over shape and morphology during the selected synthetic methods. Higher yields for photovoltaic or water splitting features have been already observed for a variety of metal oxide nanostructures<sup>[13-14]</sup>. On this basis, control of the synthetic methods for anisotropic nanomaterials, real time toxicologic observation of as-synthesized nanomaterial effects on the immune system of the living organisms which related to surface modification and their energy and clean environment applications such as photocatalysis applications have been aimed as main platform for the greener and cleaner energy solutions<sup>[15-18]</sup>.

## **1.2 Scope**

In this thesis the scientific focus was on the liquid phase room and high temperature synthesis of anisotropic ZnO and TiO<sub>2</sub> nanostructures through Hydro-solvothermal (HS), Hot Injection (HI) and Heating Up (HU) methods. A control over nucleation process that can be tuned by controlling the processing conditions (precursor concentration, temperature) as well as by extrinsic factors (addition of surfactants, seeded growth) is expected to deliver reproducible

## 1 Introduction

---

synthetic materials for controlled synthesis of functional nanomaterials. In this context, the specific objective of this doctoral thesis research were;

- i) Synthesis of ZnO, TiO<sub>2</sub> nanostructures by decomposition of different metal-organic precursors (Figure 1) followed by intrinsic encapsulation of as-formed nuclei by suitable ligands to control their shape, band gap and size

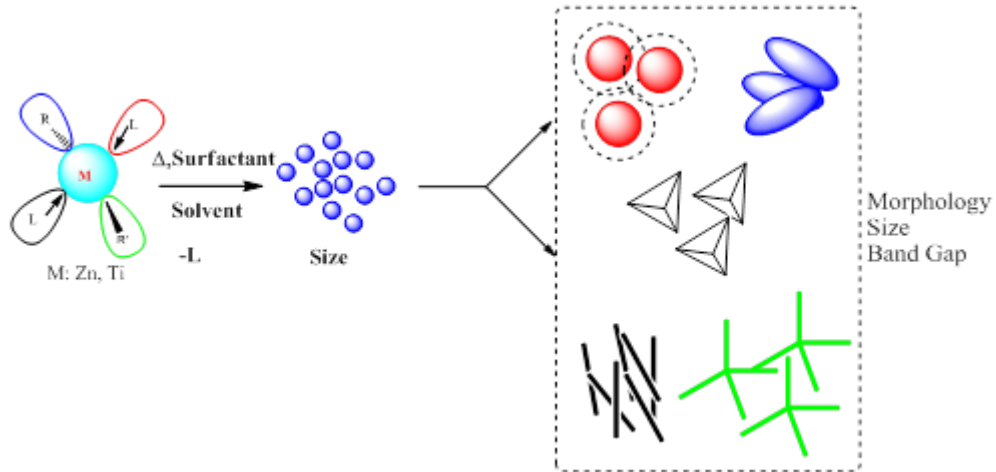


**Figure 1** General ZnO and TiO<sub>2</sub> nanostructure synthesis

- ii) Development of a library of inorganic-organic core-shell morphologies to produce Ligand@ZnO-TiO<sub>2</sub> nanostructures (Figure 2) with ligand shell and with different surface chemistry for the aim to obtain water dispersable ZnO-TiO<sub>2</sub> nanoparticles required to carry out cell tests and incorporate them into different polymer matrices

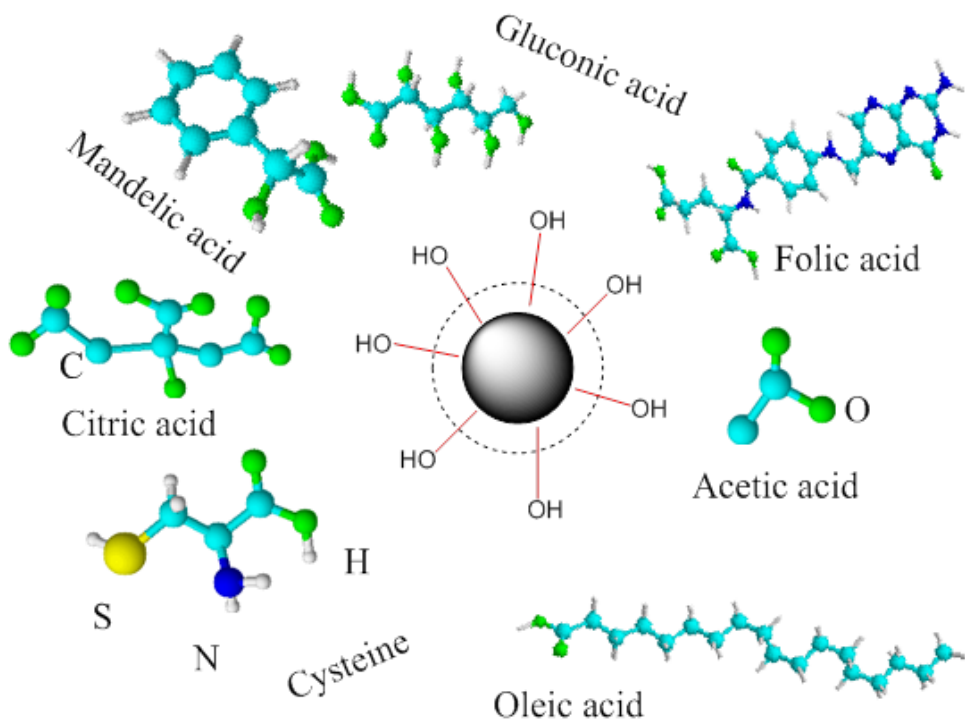


**Figure 2** Ligand library for the surface modification and core/shell protection of the nanoparticles.

iii) Phase transfer studies as the ZnO nanoparticles synthesized in organic solvent need to be transferred to aqueous and protic (e.g. alcohol) reagents to undertake evaluation of their functional properties. Within this project it was necessary to investigate the optical (emission) properties, photocatalytic behaviours and cell toxicological influence of the substituted ligands

iv) Incorporation of the ZnO and TiO<sub>2</sub> to various polymer or hybrid structures to synthesize nanocomposites based on the chemical anchoring of metal oxide nanocrystals in polymer matrices by appropriate combination of coupling chemistry. By this anchoring it is aimed to obtain superhydrophilic, broadband antibacterial, selective UV absorptive, blue to red solid state visible light emitting, biodegradable or inorganic organic nanocomposites and modulation of the photocatalytic activity and cytotoxic control have been targeted (Figure 3).

## 1 Introduction

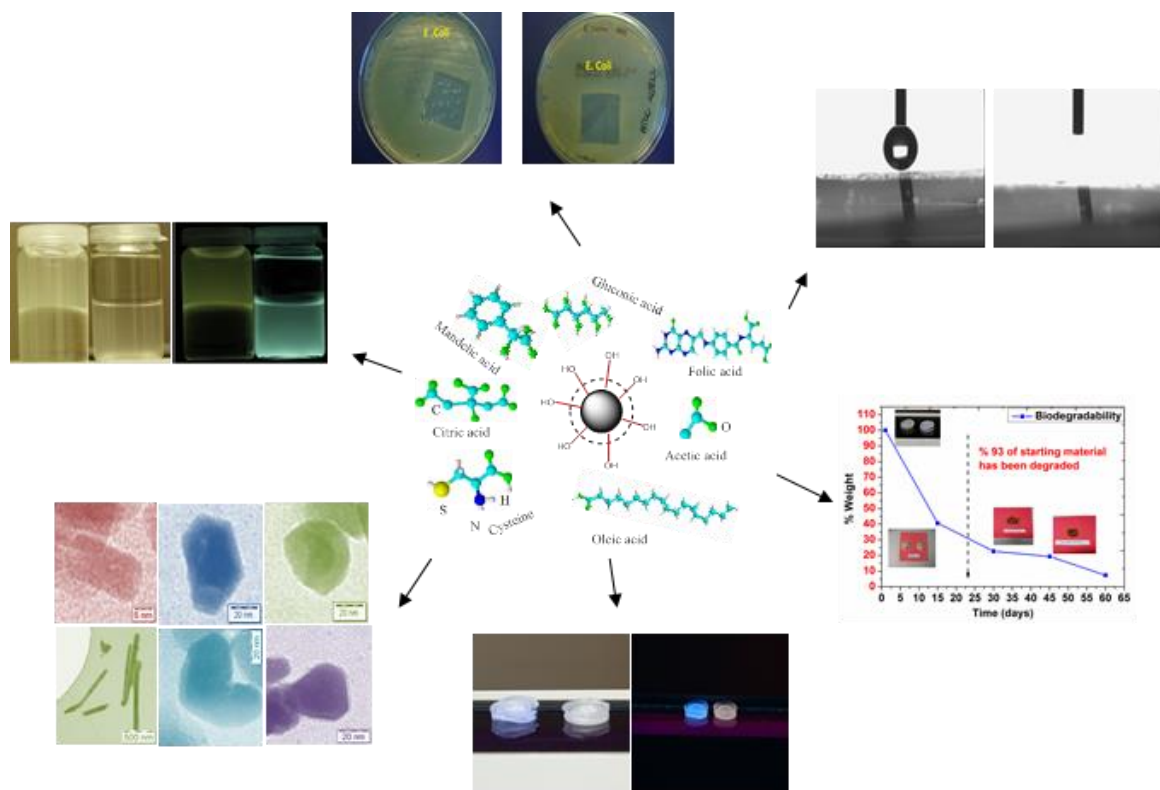


**Figure 3** Several applications of ZnO and TiO<sub>2</sub> nanostructures.

v) Multi-morphological nanoparticles of ZnO and TiO<sub>2</sub> by controlling the nucleation and growth environment. Further, the influence of surface capping agents (surfactants) will be investigated to achieve a kinetic control over the evolution of particle databases. It is known that low metal ion concentration and low degree of supersaturation promotes the formation of acicular (needle like) structure that show unique properties due to their single crystalline nature and high aspect ratio.

## 2 State-of-the-Art: Nanostructure Synthesis

### 2.1 General Concepts of Nanostructure Fabrication

Controlled synthesis of nanomaterials is achieved basically by two methods which describe their starting point to reach the final form of the nanostructures. Bottom-up method starts from a well designed molecular complex and Top-down uses a miniaturization process to fabricate the nanostructures<sup>[19]</sup>.

#### 2.1.1 Bottom-up and Top-down method

In Top-down approach, macroscopic structure can be miniaturized by applying appropriate etching and/or re-such as lithographic techniques<sup>[20]</sup>, UV light applications<sup>[21]</sup>, e-beam method<sup>[22]</sup>, nano imprinting lithography<sup>[23]</sup>, ball milling<sup>[24]</sup> and mechanic attrition<sup>[2-26]</sup>. This method found wide range applications in the commercial manufacturing processes for example electronics and daily life materials (Figure 4)<sup>[27-30]</sup>.

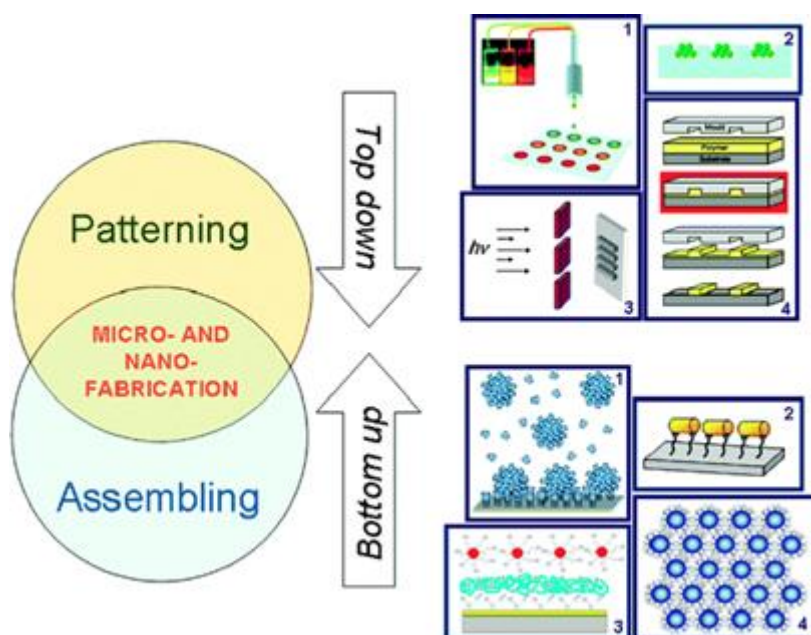


**Figure 4** (taken from ref.19 ) Scheme of complementary “top-down” and “bottom-up” approaches for fabrication of micro- and nano-structures. For the bottom-up strategies: (1) host–guest chemistry, (2) covalent immobilization onto substrate, (3) electrostatic layer-by-layer deposition, (4) self-assembly . For the top-down strategies: (1) ink jet printing, (2) capillary assembly , (3) photolithography , (4) nanoimprinting lithography [1].

On the other hand, bottom-up approach is mostly used in the fabrication of nanostructures which requires atomic precision and well characterized beginning conditions and components such as designed molecular precursors. Several subclasses of this method are present such as supramolecular self-assembly<sup>[31]</sup>, surface directed ordering at interfaces (liquid crystals; LC)<sup>[32]</sup>, Langmuir–Blodgett (LB) synthesis method<sup>[33]</sup>, chemical vapour synthesis<sup>[34]</sup>, liquid phase methods<sup>[35-36]</sup> (hot injection, microwave), combustion methods<sup>[37-38]</sup>.

## 2.2 La-Mer theory for the nanoparticle formation: Nucleation and Growth

Solution based production of nanocrystals follow two important steps; a) nucleation and b) growth of the nanocrystals. These processes are widely investigated and formulated.

La Mer and coworkers studied nucleation and growth of sulphur based structures and developed a theory which covers the formation of nanocrystals from homogeneous, supersaturated conditions. According to their mechanism synthesis of the colloid structure should be arranged in a way that the concentration of initial species increases rapidly and rising above the required saturation concentration for a short period of time so that the fast burst of nucleation occurs with the formation of a large number of nuclei in a short time. Particle growth is extremely fast and therefore lower the concentration below the nucleation level slowest step in the growth process.

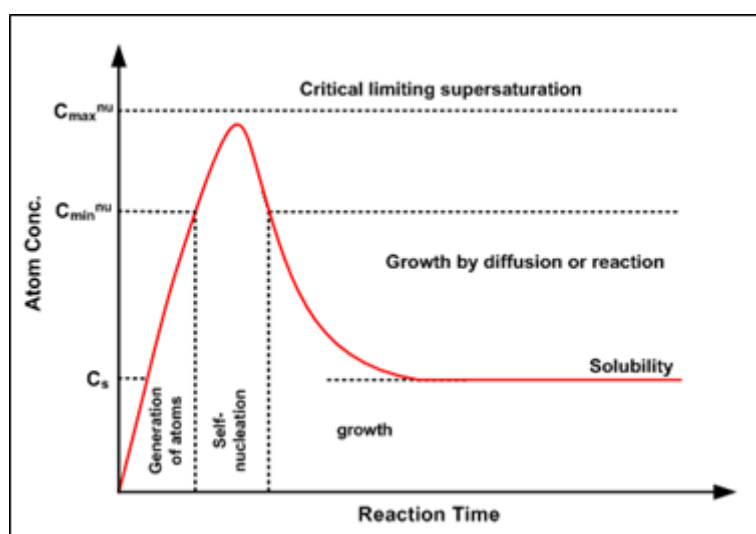


**Figure 5** Schematic diagram illustrating La Mer's condition for stable nucleation<sup>[39]</sup>.